STEM CELLS®
EMBRYONIC STEM CELLS

Gap Junctions and Connexon Hemichannels in Human Embryonic Stem Cells

JAMES E. HUETTNER,[a] AIWU LU,[a,b,c,d] YUN QU,[b,c,d] YINGJI WU,[b,c,d] MIJEONG KIM,[a] JOHN W. MCDONALD[b,c,d,e]

[a]Department of Cell Biology and Physiology, [b]Department of Neurology, [c]Department of Neurological Surgery, [d]Spinal Cord Injury Restorative Treatment and Research Program, [e]Department of Anatomy and Neurobiology, Washington University School of Medicine, St. Louis, Missouri, USA

Key Words. Connexin • Dye coupling • Electron microscopy • Patch clamp • Reverse transcription-polymerase chain reaction

ABSTRACT

Intercellular communication via gap junctions is thought to play an important role in embryonic cell survival and differentiation. Classical studies demonstrated both dye and electrical coupling of cells in the inner cell mass of mouse embryos, as well as the development of restrictions against coupling between cells of the inner cell mass and surrounding trophectoderm. Here we demonstrate extensive gap junctional communication between human embryonic stem (ES) cells, the pluripotent cells isolated from the inner cell mass of preimplantation blastocysts. Human ES cells maintained in vitro expressed RNA for 18 of the 20 known connexins; only connexin 40.1 (Cx40.1) and Cx50 were not detected by reverse transcription-polymerase chain reaction. Cx40, Cx43, and Cx45 were visualized by immunofluorescence at points of contact between adjacent cells. Electron microscopy confirmed that neighboring cells formed zones of tight membrane apposition characteristic of gap junctions. Fluorescent dye injections demonstrated extensive coupling within human ES cell colonies growing on mouse embryonic fibroblast (MEF) feeder cells, whereas dye coupling between human ES cells and adjacent MEFs was extremely rare. Physiological recordings demonstrated electrical and dye coupling between human ES cells in feeder-free monolayers and between isolated human ES cell pairs. Octanol, 18-α-glycyrrhetinic acid, and arylaminobenzoates inhibited transjunctional currents. Dye uptake studies on human ES cell monolayers and recordings from solitary human ES cells gave evidence for the surface expression of connexon hemichannels. Human ES cells provide a unique system for the study of human connexin proteins and their potential functions in cellular differentiation and the maintenance of pluripotency. STEM CELLS *2006;24:1654–1667*

INTRODUCTION

Gap junction channels mediate electrical and biochemical communication in a wide variety of somatic cells and tissues [1]. Electrical coupling within cardiac and smooth muscle, metabolic coupling in the lens, and potassium homeostasis within glial cell networks in the nervous system all depend on transmission through gap junctions [2]. In addition, gap junction channels underlie the extensive intercellular communication that is observed in early embryos [3, 4].

More than 20 different connexin (Cx) subunits that contribute to vertebrate gap junction channels have been cloned and characterized [5]. Formation of a gap junction involves the end-to-end coupling of two connexon hemichannels, each composed of six connexin subunits, within the surface membranes of adjacent cells. It was long believed that hemichannels outside gap junctions remained closed. However, more recent work indicates that currents or small molecules passing through isolated surface hemichannels may have important biological functions [6].

In rodents, expression of zygotic connexin genes, including *cx31, cx40,* and *cx43,* begins as early as the two- to four-cell stage [7, 8]. Widespread coupling throughout the embryo is prominent from compaction at the eight-cell stage through to implantation [3]. Following implantation, cells of the inner cell mass remain coupled to each other, but they lose gap junction-mediated transmission of dye to cells of the surrounding trophectoderm [4]. Further restrictions in coupling arise as development proceeds. Coupling diminishes across the boundaries between germ layers, although cells within each germ layer remain well coupled to each other [9]. These patterns ofcommunication are thought to be important in the regulation of

Correspondence: James E. Huettner, Ph.D., Dept. of Cell Biology & Physiology, Washington University Medical School, 660 South Euclid Avenue (Campus Box 8228), St. Louis, Missouri 63110, USA. Telephone: 314-362-6624; Fax: 314-362-7463; e-mail: huettner@cellbio.wustl.edu; or John W. McDonald III, M.D., Ph.D., Kennedy Krieger Institute, International Center for Spinal Cord Injury, 707 North Broadway, Room 518, Baltimore, Maryland 21205, USA. Telephone: 443-923-9210; Fax: 443-923-9215; e-mail: mcdonaldj@kennedykrieger.org Received January 5, 2005; accepted for publication March 30, 2006; first published online in STEM CELLS *EXPRESS* March 30, 2006. 1066-5099/2006/$20.00/0 doi: 10.1634/stemcells.2005-0003

embryonic development, but identifying the salient molecules exchanged through gap junctions early in development has proven difficult.

Pluripotent mammalian embryonic stem (ES) cells, which are derived from the inner cell mass of preimplantation blastocysts, have the capacity to differentiate into cells of all three germ layers [10]. Under suitable conditions, ES cells remain pluripotent through repeated rounds of cell division in culture [11]. The recent isolation of human ES cells [12] has spurred great interest in their potential use for therapeutic tissue repair because appropriate manipulation of the culture environment can induce both mouse and human ES cells to differentiate in vitro into specific somatic cell types [13]. Although brief reports of connexin expression by mouse [14] and human [15–17] ES cells have appeared, the physiological properties of human ES cell gap junctions have not been characterized. Moreover, the roles that gap junctions play in the process of differentiation remain poorly understood.

In the present study, we demonstrate the formation of gap junction channels between human ES cells maintained in vitro. Our results show that human ES cells express RNA encoding most of the known human connexin genes. Electrical and dye coupling is prominent in human ES cell colonies and monolayers and between individual pairs of cells. In addition, human ES cells exhibit currents and dye loading from calcium-free solutions that are characteristic of connexon hemichannels present on the surface membrane. Thus, human ES cells provide a useful system for studying the role of human gap junctional communication during development and cellular differentiation.

Materials and Methods

Mouse Embryonic Fibroblast Feeder Layer

Mouse embryonic fibroblast (MEF) feeder layers were prepared in a modification of previously published protocols [15, 18, 19]. Briefly, pregnant CD1 strain mice were sacrificed by CO_2 asphyxiation. Male and female embryos were dissected and eviscerated under sterile conditions. The tissue was minced and triturated in 0.25% trypsin/EDTA (Gibco, Grand Island, NY, http://www.invitrogen.com) to a single-cell suspension and plated at a density of 0.5–1.0 embryo equivalents per 75-cm^2 flask containing Dulbecco's modified Eagle's medium (DMEM) (HyClone, Logan, UT, http://www.hyclone.com), supplemented with 2 mM glutamine, 0.1 mM nonessential amino acids (Gibco), and 10% fetal bovine serum (FBS) (HyClone). Medium was changed every other day. MEFs were harvested on day 3 by trypsinization and frozen as stocks using dimethyl sulfoxide (DMSO). Frozen stocks were thawed and plated in 75-cm^2 flasks in complete medium at a density of 1.0×10^6 ml^{-1}. Cell division was inhibited by the addition of 10 μg ml^{-1} mitomycin C (Sigma-Aldrich, St. Louis, http://www. sigmaaldrich.com) for 2.5 hours on day 3. Cells were washed, retrypsinized to a single-cell suspension, and replated at a density of 1.0×10^6 cells ml^{-1} in 35-mm dishes or 24-well plates. Human ES cells were plated onto MEFs during the succeeding 2 days to 2 weeks.

Human ES Cell Culture

Two lines of human ES cells were used in completing these studies: one donated by BresaGen (NIH code, BG01; provider's code, human ESBGN.01; passage 42; BresaGen, Athens, GA) and the other purchased from WiCell Research Institute (NIH code, WA01; provider's code, H1; passage 24; WiCell Research Institute, Madison, WI, http://www.wicell.org) and maintained according to the providers' protocols [12, 15, 20–22]. Chromosome counts confirmed normal complements of 46XY (BG01/ESBGN.01) [21] and 46XX (WA01/H1) [12, 20] and chromosome number stability within each cell line. Studies were carried out on human ES cells with passage numbers ranging from 50 to 72 (BG01) and from 35 to 50 (WA01). Similar data were obtained with both cell lines, but for simplicity, all data presented in this report represents the BresaGen cell line (BG01). Undifferentiated human ES cells were maintained on a preexisting feeder layer of MEFs (passage 2). The human ES cell culture medium consisted of 80% DMEM/Ham's F-12 medium (Gibco), 15% FBS (Hyclone), 5% knockout serum replacement (Gibco), 2.0 mM L-glutamine (Gibco), 0.1 mM nonessential amino acids (Gibco), 4 ng ml^{-1} basic fibroblast growth factor (Sigma-Aldrich), and 0.1 mM β-mercaptoethanol (Sigma-Aldrich). Cell cultures were incubated at 37°C in 5% CO_2 in air and 95% humidity. After 3–4 days, phosphate-buffered saline (PBS)-based cell dissociation buffer (Gibco) was used to lift visually identified colonies of undifferentiated human ES cells off the feeder layer for passage to a new dish of feeder cells. Feeder-free cultures of undifferentiated human ES cells were prepared by transferring human ES cells isolated from feeder layers into feeder-free 35-mm dishes or glass-covered 24-well plates containing human ES cell-conditioned medium. The density of seeding human ES cells was estimated to be 6.0×10^4 ml^{-1} to 1.0×10^5 ml^{-1}, based on counts of individual cells and small-cell clumps obtained after gentle trituration of isolated human ES cell colonies. For most experiments, contamination by MEF feeder cells was minimized by passaging feeder-free cultures two to four additional times, at 2–3-day intervals, before use. Human ES cell-conditioned medium was collected daily from cultures that contained feeder cells by removing all of the medium from each culture and replacing it with fresh medium. Plates or dishes were incubated with human ES cell-conditioned medium for 30 minutes before use [23].

Chromosome Counts

Chromosome counts of cell line BG01 were performed between passage 50 and passage 72. The cells were grown to 70% confluence in a 25-cm flask and fed with medium containing colcemide (final concentration, 0.02 μg ml^{-1}) 1 hour prior to analysis. Cells were washed with PBS, trypsinized for 5 minutes, and collected by centrifugation (70g, 3 minutes) in a conical tube. Cells were incubated for 6 minutes at room temperature in 5 ml of hypotonic (0.56%) KCl and then fixed by five changes of methanol/acetic acid (3:1; total volume, 1 ml). To create cell spreads, the cell suspension was dropped from at least 1 foot above the surface of the slide and allowed to air dry. Slides were stained with Giemsa for at least 15 minutes, washed with running water for 1 minute, and air-dried. Chromosome spreads were photographed, and representative photos were used to provide chromosomal counts.

Reverse Transcription-Polymerase Chain Reaction

Total RNA was prepared from human ES cells and from MEF cultures using the RNeasy mini kit (Qiagen, Hilden, Germany, http://www1.qiagen.com). Small amounts of contaminating DNA were removed by treatment of the RNA samples with RNase-free DNase I (Promega, Madison, WI, http://www.

Table 1. Primers for reverse transcription-polymerase chain reaction [5]

Connexin	Accession number	Forward and reverse primers	Product size (bp)
Cx25	NM_198568	GGATGGATTTGGCTGGCTGTCGTGTTTG ATAAGCGTACCATAGGCCCCCATCCATTGT	312
Cx26	NM_004004	GACGCAGAGCAAACCGCCCAGAGTAGAAG ATAGCCGGATGTGGGAGATGGGGAAGTAGTGA	258
Cx30	NM_006783	GGGCCCTCCAGCTGATCTTCGTCTCC TTACTCTCCTTTAGGGCATGATTGGGGTGATTTTTT	490
Cx30.2 (29)	NM_181538	GGCGCCTCTTGCTTCCCGTGCTCCT GGTCTCCTCCTCCTTCCCCTTTCCTGATAAT	281
Cx30.3	NM_153212	CCGCATCTGGCTGTCTGTGGTGTTCATCTTT ACGCGGGGCATGTCATAATCCTTGTAGAG	420
Cx31	NM_024009	TGGGCCCTGCAGCTCATCTTCGTCACA CTTCTCGGTAGGTCGGGCAATGTAGCAGTCC	324
Cx31.1	NM_005268	GAACAGTGGGCGCCTCTACCTGAAC GGCAGCCCCTCACAAGATGGTTTTC	499
Cx31.9	NM_152219	CGCGCCTTCCCGGTCTCCCACTAC CCCCACCGCGAAATAGAAGAGCACGAAGAC	393
Cx32	NM_000166	GAATGAGGCAGGATGAACTGGACAGGTTTG GGGGCAGGGGTAGACGTCGCACTTGA	534
Cx36	NM_020660	TACCCCCAGTCTTTGCTTCATCACCTAC AGTCTTCTCAGTTGGCCGGGACACA	493
Cx37	NM_002060	GCATCCGCGGAGCACTGA GGGGGTTTTTGGCCATTCTGAGG	523
Cx40	NM_005266	AGGTCCGGGGCTCTGGCTCTTACGA GGGGGTGGTGTGCAGCTCTGGACTATG	448
Cx40.1	NM_153368	GACTTTTCGGCCGGCTACATCATCCAC GCGCCGGTGCCCCCTCTTCCT	382
Cx43	NM_000165	GGGGCAGGCGGGAAGCACCATCTC TCTCTTATCCCCTCCCTCTCCACCCATCTACCC	396
Cx45	NM_005497	GCCAACACAGCCCAGGAACAGCAGTATG AAGCACAGGTTTTAAGCCCGCCAGGATT	272
Cx46	NM_021954	ATCGTGCGCATGGAAGAGAAGAAGAAAGAGA AGGGGCGGGGGATCGGCTGTCC	470
Cx47	NM_020435	GCCCGCCCGCCCCTATGA CCAGGTCGGCGGGCTCAG	438
Cx50	NM_005267	TCCCGGGGCTACCAAGAGACACTG CCTGGCTCGGCTGCTGGCTTTGCTTAG	345
Cx59	NM_030772	AGCGACTCCCTTCTGCCCCTGATTAT GGTTCTGACTGTGCCCTTTCTGA	536
Cx62	NM_032602	ATGCGGTGGATTGCTTTGTAT AGTTGCCTTGGCTGTGGGATTT	346

Abbreviations: bp, base pair(s); Cx, connexin.

promega.com) according to the manufacturer's instructions. Two micrograms of total RNA was used to prepare single-strand cDNA. Omniscript reverse transcriptase (Qiagen) was used for reverse transcription following the manufacturer's instructions. Polymerase chain reactions (PCRs) were performed according to Di et al. [24], with some modification using HotStarTaq DNA polymerase (Qiagen). Primers for PCR, which are listed in Table 1, were chosen using the PrimerSelect module of Lasergene (DNAStar, Madison, WI, http://www.dnastar.com) based on their specificity among homologous human connexins and their selectivity for human versus mouse connexin sequences. The PCR program was 94°C for 15 minutes to activate the dormant polymerase; followed by 32–36 cycles of 94°C for 1 minute, 60°C for 1 minute (55°C for Cx59 and Cx62), and 72°C for 1 minute; and completed with a final extension of 72°C for 10 minutes. As all paired primers lie within a single exon (most connexins are encoded in a single exon), a negative control for each reverse transcription-polymerase chain reaction (RT-PCR) was run using the same conditions but without reverse transcriptase to eliminate the possibility of genomic DNA contamination. In a 50-μl reaction mixture, 2 μl of 1 ng/μl human placenta DNA (Sigma-Aldrich) was used as a positive control. All primer pairs were also tested in PCRs with mouse genomic DNA (not shown) and MEF cell cDNA to rule out spurious amplification of mouse connexin sequences. RT-PCR products were separated on 1.5% agarose gels. The gels were stained with ethidium bromide and visualized by UV transillumination (Spectroline, Westbury, NY, http://www.spectroline.com). PCR products amplified from human ES cell cDNA were cut from the gel and partially sequenced to verify their identity.

Immunofluorescence

To visualize connexins, human ES cell cultures were washed and fixed with 4% paraformaldehyde plus 0.025% glutaraldehyde in 0.12 M sodium phosphate buffer, pH 7.4. Cultures were

Table 2. Antibody antigen characteristics

Primary antibody	Antibody type	Labeling identity [33]	Dilution	Source
SSEA-1	mIgM	Carbohydrate antigen expressed by mouse ES cells	1:50	DSHB[a] (MC-480)
SSEA-3	mIgM	Glycolipid antigens with globoseries carbohydrate core structures expressed by early ES cells	1:50	DSHB (MC-631)
SSEA-4	mIgG3	Glycolipid carbohydrate epitope expressed by early ES cells	1:50	DSHB (MC-813–70)
TRA-1-60	mIgM	Keratin sulfate-associated antigen, sialidase-sensitive epitope	1:50	Chemicon[b] (MAB4360)
TRA-1-81	mIgM	Pericellular matrix proteoglycan	1:50	Chemicon (MAB4381)
Oct3/4	Rabbit polyclonal	The first 134 amino acids of recombinant human Oct3/4	1:200	Santa Cruz[c] (SC-9081)
Human nuclear antigen	mIgG1	Nuclear staining of all human cell types	1:100	Chemicon (MAB1281)
Connexin 40	Rabbit polyclonal	19-amino acid peptide sequence within C-terminal cytoplasmic domain of Cx40	1:100	Chemicon (AB1726)
Connexin 43	Rabbit polyclonal	23-amino acid C-terminal peptide sequence within the cytoplasmic domain of Cx43	1:100	Chemicon (AB1728)
Connexin 45	Rabbit polyclonal	Carboxy terminal of Cx45	1:1,000	T.H. Steinberg

[a] Developmental Studies Hybridoma Bank (DSHB), Iowa City, IA, http://www.uiowa.edu/~dshbwww (antibodies developed by D. Solter).
[b] Chemicon, Temecula, CA, http://www.chemicon.com.
[c] Santa Cruz Biotechnology Inc., Santa Cruz, CA, http://www.scbt.com.
Abbreviations: Cx, connexin; ES, embryonic stem; SSEA, stage-specific embryonic antigen; TRA, tumor rejection antigen.

rinsed with PBS, permeabilized in 0.1% Triton X-100, and blocked in 10% normal goat serum in PBS. Cultures were incubated for 1 hour at room temperature or overnight at 4°C with primary antibodies (Table 2) anti-Cx40 and Cx43 at 1:100 dilution and anti-Cx45 [25, 26] at 1:1,000 dilution. Cultures were then washed in PBS and incubated for 1 hour at room temperature with Cy3-conjugated goat anti-rabbit immunoglobulin at 1:100 dilution. Cell nuclei were counterstained with Hoechst 33342. Specimens were imaged using a Nikon microscope equipped with differential interference contrast microscopy optics, fluorescence epi-illumination, a cooled charge-coupled device camera (Cooke Corp. Ltd., Romulus, MI, http://www.cookecorp.com), and Metamorph acquisition software.

For surface antigen immunofluorescence, cells were fixed with 4% paraformaldehyde in 0.12 M sodium phosphate buffer, pH 7.4, blocked with 10% normal goat serum in PBS and incubated at room temperature for 1 hour in primary antibodies at 1:50 dilution (Table 2). Cultures were washed with PBS and incubated at room temperature for 1 hour with 1:100 dilutions of fluorescein isothiocyanate- or Cy3-conjugated goat anti-mouse IgG or IgM, as appropriate (Table 2).

For double immunofluorescence of rabbit anti-Oct3/4 and mouse anti-human nuclear antigen (Table 2), cells were fixed with 4% paraformaldehyde in 0.12 M sodium phosphate, pH 7.4, rinsed with PBS, permeabilized with 0.1% Triton X-100, and blocked with 10% normal goat serum. Cultures were incubated simultaneously with anti-Oct3/4 (1:200) and anti-human nuclear antigen (1:100) for 1 hour at room temperature. Cells were then rinsed and incubated for 1 hour at room temperature in a mixture of Cy2-conjugated goat anti-mouse IgG and Cy3-conjugated goat anti-rabbit immunoglobulin, both at 1:200 final dilution. Preliminary single immunofluorescence control experiments confirmed the specificity of the secondary antibodies and the adequacy of our filter set to prevent spillover between the Cy2 and Cy3 channels (data not shown).

Electron Microscopy

Feeder-free human ES cells, prepared as described above, were fixed at 5 days in vitro with 2.5% glutaraldehyde in 0.1 M PBS, postfixed in 1% OsO_4, block-stained with 1% uranyl acetate, dehydrated in ethanol, and then embedded in polybed 812. Thin sections were cut and stained with uranyl acetate and lead citrate and then examined using a JEOL 100CX transmission electron microscope.

Electrophysiology

Whole-cell recordings were obtained with borosilicate glass pipettes. Passive properties and resting membrane potentials were evaluated using electrodes filled with (in mM) 140 potassium glucuronate, 5 KCl, 10 EGTA, 5 magnesium-ATP, 1 Tris-GTP, and 10 HEPES, pH adjusted to 7.4 with KOH. The open-tip resistance ranged from 1 to 3 MOhm. The bath was perfused at 1–2 ml/minutes with Tyrode's solution (in mM) 150 NaCl, 4 KCl, 2 $MgCl_2$, 2 $CaCl_2$, 10 D-glucose, and 10 HEPES adjusted to pH 7.4 with NaOH. After seal formation in the Tyrode's bath, a wide-bore (300 μm) multichannel delivery pipette was positioned to provide local perfusion of various external solutions. Currents were recorded with Axoclamp 200B and/or 200A amplifiers (Axon Instruments/Molecular Devices Corp., Union City, CA, http://www.moleculardevices.com), filtered at 1–5 KHz with the internal Bessell filter of the clamp, and digitized at 10–50 KHz. In-house software controlled the voltage commands and data acquisition to disc. Recordings were accepted for analysis if the seal resistance before breakthrough

exceeded 1 GOhm. Immediately after breaking through to the whole-cell configuration the input resistance, series resistance and membrane capacitance were determined from the average of currents recorded during six hyperpolarizing voltage steps. In addition to the potassium glucuronate intracellular and Tyrode's extracellular solutions described above, permeation through surface hemichannels was evaluated using internal and external solutions of the following compositions.

Internal Solutions.

Cesium glucuronate: 140 mM cesium glucuronate, 5 mM CsCl, 5 mM magnesium-ATP, 1 mM Tris-GTP, 10 mM EGTA, 10 mM HEPES; pH adjusted to 7.4 with CsOH.

N-Methyl-D-glucamine chloride: 140 mM *N*-methyl-D-glucamine (NMDG) chloride, 5 mM magnesium-ATP, 1 mM Tris-GTP, 0.1 mM EGTA, 10 mM HEPES; pH adjusted to 7.4 with *N*-methyl-D-glucamine.

Tetraethylammonium chloride: 120 mM tetraethylammonium (TEA) chloride, 5 mM $MgCl_2$, 5 mM magnesium-ATP, 1 mM Tris-GTP, 10 mM EGTA, 10 mM HEPES; pH adjusted to 7.4 with TEA hydroxide.

External Solutions.

NaCl: 160 mM NaCl, 1 mM calcium glucuronate, 10 mM HEPES; pH adjusted to 7.4 with NaOH.

Sodium glucuronate: 160 mM sodium glucuronate, 1 mM calcium glucuronate, 10 mM HEPES; pH adjusted to 7.4 with NaOH.

NMDG-chloride: 160 mM *N*-methyl-D-glucamine chloride, 1 mM Ca-glucuronate, 10 mM HEPES; pH adjusted to 7.4 with *N*-methyl-D-glucamine.

NMDG-glucuronate: 160 mM *N*-methyl-D-glucamine *d*-glucuronate, 1 mM Ca-glucuronate, 10 mM HEPES; pH adjusted to 7.4 with *N*-methyl-D-glucamine.

Calcium-free: 160 mM NaCl, 0.5 mM EGTA, 10 mM HEPES; pH adjusted to 7.4 with NaOH.

In these solutions, small inorganic cations (sodium and cesium) or anions (chloride) are replaced by larger organic cations (TEA, NMDG) or anions (glucuronate), which should pass through the large diameter connexon pore but be impermeable through most conventional voltage-gated ion channels [27]. Mean ± SEM values are reported for all measured parameters. Statistical significance was assigned for $p < .05$.

Dye Injections

Whole-cell electrodes were used to inject individual cells with fluorescent dyes dissolved in the same internal solution used for electrophysiology experiments. Initially sulforhodamine B (555 Da; Sigma-Aldrich) or Lucifer Yellow CH (443 Da; Sigma-Aldrich) were injected at 0.4%; however, most experiments used aldehyde-fixable AlexaFluor hydrazides. AlexaFluor 488 (570 Da) and 568 (731 Da) hydrazides were purchased as 10 mM solutions in 200 mM KCl (Molecular Probes Inc., Eugene, OR, http://probes.invitrogen.com) and were diluted 1:100 into internal solution. For some experiments, AlexaFluor 568 hydrazide was co-injected with Lucifer Yellow coupled to 10 kDa anionic dextran, which is too large to pass through gap junction channels and therefore remains within the injected cell. Cells injected with fluorescent hydrazides were imaged live and in some cases were also fixed for subsequent immunofluorescence. Cultures were fixed in 0.12 M sodium phosphate buffer, pH 7.4, containing 4% paraformaldehyde alone to preserve antigenicity for Oct3/4 and the human nuclear antigen, although our preliminary experiments revealed superior retention of fluorescent AlexaFluor hydrazides by cells that were fixed with a mixture of 4% paraformaldehyde and 0.1% glutaraldehyde.

Pharmacological Agents

Compounds previously demonstrated to inhibit electrical or dye coupling between cells [1] or to block hemichannel-mediated currents [6] were dissolved in external solution and delivered to cells by local perfusion from a mutibarrelled pipette. Octanol [1] (Sigma-Aldrich) was diluted directly into the extracellular solution. Cobalt and lanthanum (Sigma-Aldrich), which inhibit currents mediated by hemichannels [28, 29], were prepared as 0.1 M stocks in water. The arylaminobenzoates niflumic acid and flufenamic acid [6, 30] and the aglycone from licorice (*Glycyrrhiza glabra*) root, 18-α-glycyrrhetinic acid [31], and its synthetic analog, carbenoxylone [31], were purchased from Sigma-Aldrich and prepared as 50 mM stocks in DMSO. Addition of 0.2% DMSO alone was found to have no effect on currents through gap junctions or hemichannels.

Results

Undifferentiated human ES cells were maintained on MEFs (Fig. 1A) and were also grown independent of feeder cells using a modification of previously described protocols [23] (Materials and Methods). Cells were passaged every other day and maintained at high density (Fig. 1B). Low passage numbers from frozen stocks were used for most experiments. Under these conditions, the cells retained a normal chromosome count (Fig. 1C) and expressed the stage-specific embryonic antigen 3 (SSEA-3) (not shown), SSEA-4, TRA-1-60, and TRA-1-81 (Fig. 1D–1F) surface antigens, but not the SSEA-1 antigen, an antigen expression pattern that is diagnostic of pluripotent human ES cells prior to differentiation [19, 23, 32, 33]. To confirm preservation of the undifferentiated phenotype as human ES cells were passaged to feeder-free conditions, we performed double immunofluorescence for the Oct3/4 transcription factor [34, 35], a definitive marker of undifferentiated human ES cells [36], and for a human cell-specific nuclear antigen [37], which allowed for unambiguous discrimination between human ES cells and any contaminating mouse cells. As illustrated in Figure 1G–1J, strong nuclear expression of Oct3/4 was maintained in human ES cells but was not observed in the rare MEFs that survived through initial passages to feeder-free dishes.

Connexin Expression in Human ES Cells

As an initial screen for the production of gap junction constituents by human ES cells, we evaluated expression of connexin mRNA by RT-PCR (Fig. 2). In replicate experiments from four separate platings, PCR products were observed for nearly all of the known human connexins (Table 1). Only Cx40.1 and Cx50 were not detected in any samples from undifferentiated human ES cell. Strong PCR products were observed for Cx25, Cx26, Cx30.3, Cx31, Cx31.1, Cx31.9, Cx37, Cx40, Cx43, Cx45, and Cx46 for all of the undifferentiated human ES cultures that were sampled. The remaining connexins (Cx30, Cx30.2, Cx32, Cx36, Cx47, Cx59, and Cx62) were also reliably detected in undifferentiated human ES cells but yielded weaker PCR product bands in some of the replicate experiments.

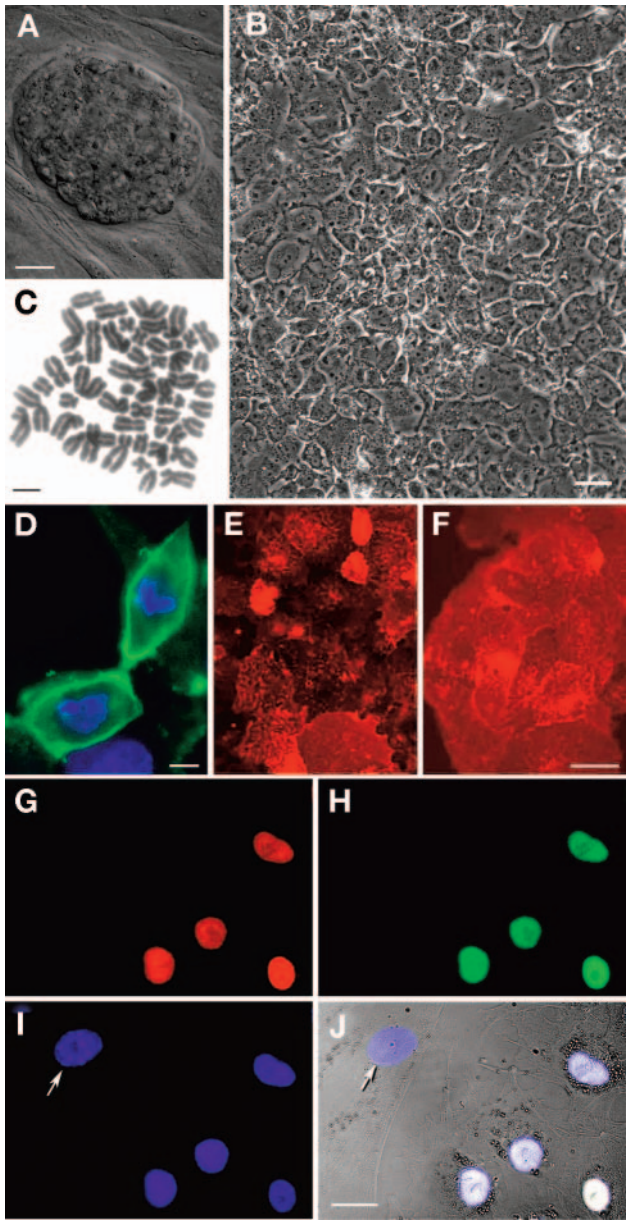

Figure 1. Human embryonic stem (ES) cells in culture. **(A):** Differential interference contrast (DIC) microscopy image of human ES cells clustered on a mouse embryonic fibroblast (MEF) feeder layer. **(B):** Phase contrast image of a feeder-free human ES cell monolayer. **(C):** Interphase chromosome spreads from feeder-free human ES cells after 56 total passages, the final four passages under feeder-free growth conditions. **(D–F):** Immunofluorescent visualization of stage-specific embryonic antigen-4 (green) **(D)**, TRA-1-81 (red) **(E)**, and TRA-1-60 (red) **(F)** antigens in feeder-free human ES cells monolayers. **(G–J):** Double immunofluorescence for Oct3/4 (red) **(G)** and human nuclear antigen (green) **(H)** together with Hoechst 33342 nuclear counterstaining (blue) **(I)**, which reveals an MEF nucleus (arrow). **(J):** Composite of **(G–I)** with the DIC image of the same field. Scale bars = **(A)**, 30 μm; **(B)**, 10 μm; **(C)**, 3 μm; **(D)**, 10 μm; and **(E, F, G–J)**, 30 μm.

To test for production of connexin proteins and to visualize their subcellular distribution, we performed immunofluorescence on human ES cell monolayers (Fig. 3A–3C). Antibodies to Cx40, Cx43, and Cx45 [25, 26] revealed a pattern of bright punctate spots and extended segments of fluorescence along the

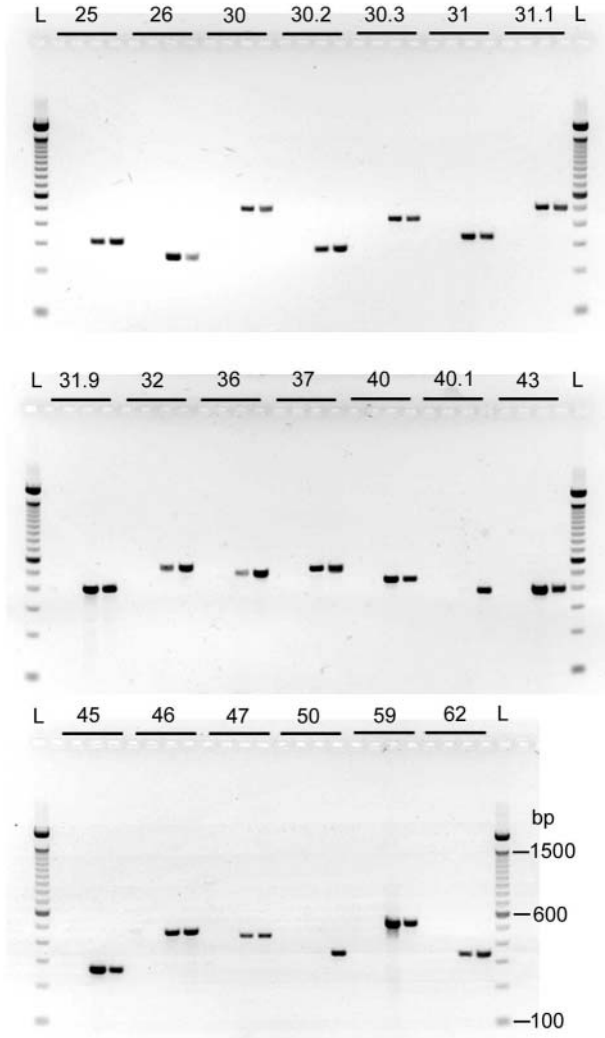

Figure 2. Reverse transcription (RT)-polymerase chain reaction (PCR) analysis of connexin expression in undifferentiated human embryonic stem (ES) cells. Experiments were performed as outlined in Materials and Methods using PCR primers in Table 1. For each connexin, four lanes were run in the following order: lane 1, PCR using reverse-transcribed mouse embryonic fibroblast (MEF) cDNA; lane 2, PCR of the RT-negative control in which DNase-treated total RNA from human ES cells was used without reverse transcriptase to rule out the possibility of genomic DNA contamination; lane 3, PCR using reverse-transcribed human ES cell cDNA; lane 4, PCR using human placenta genomic DNA as a positive control. PCR products were detected for all 20 of the positive controls but not for any of the MEF cDNA or RT-negative control lanes. Abbreviations: bp, base pairs; L, 100-base pair DNA size ladder.

borders between neighboring cells. Regions of tight membrane apposition, which are characteristic of gap junctions [38], were confirmed by transmission electron microscopy (Fig. 3D–3F). The density of tight membrane appositions was greater in samples from near-confluent high-density cultures than in similar samples from low-density cultures.

Physiology and Dye Coupling of Human ES Cells

To characterize the physiology of human ES cells and to provide an initial test for gap junction-mediated communication between cells, we obtained whole-cell recordings from 33 human ES

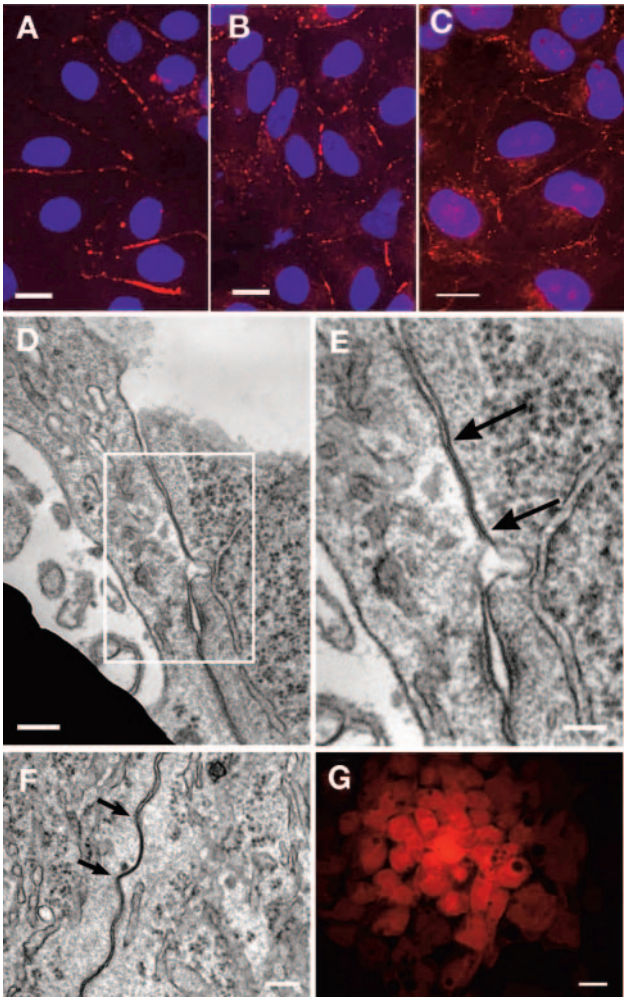

Figure 3. Gap junction distribution and function in human embryonic stem (ES) cells. Distribution of Cx40 **(A)**, Cx43 **(B)**, and Cx45 **(C)** in human ES cells visualized by immunofluorescence (red). Nuclei counterstained with Hoechst dye (blue). **(D–F):** Transmission electron micrographs of human ES cells. Arrows indicate regions of close membrane apposition characteristic of gap junctions. **(E):** Higher power view of the region boxed in **(D)**. **(G):** Dye coupling between human ES cells revealed by spread from the cell indicated by the asterisk, which was injected with sulforhodamine B through a whole-cell electrode. Scale bars = **(A–C)**, 20 μm; **(D, F)**, 200 nm; **(E)**, 100 nm; and **(G)**, 30 μm.

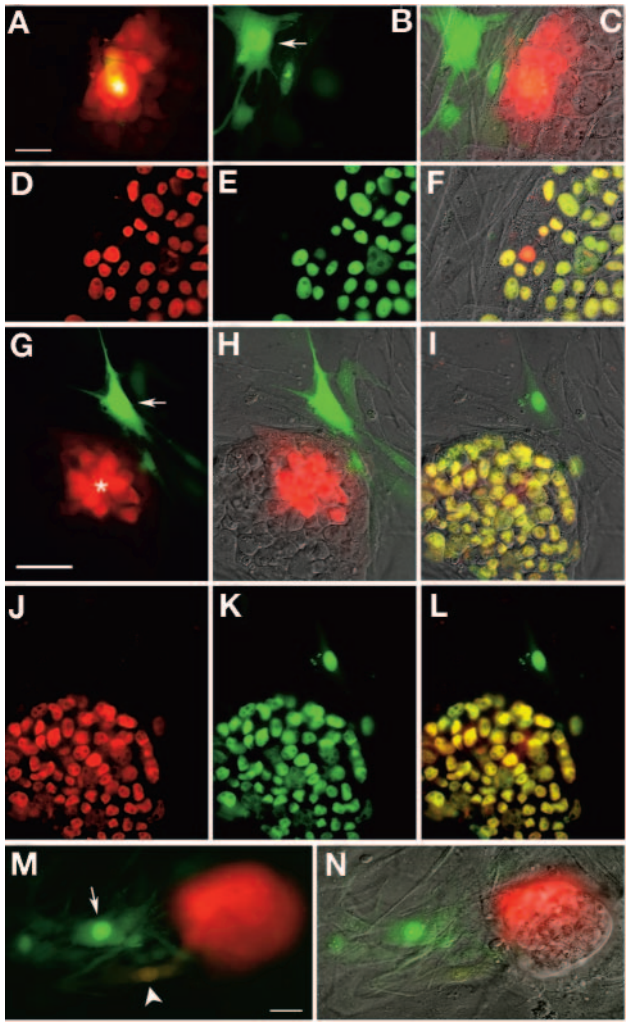

Figure 4. Lack of dye coupling between human embryonic stem (ES) cells and mouse feeder cells. **(A):** AlexaFluor 568 hydrazide (731 Da; red) delivered into a single human ES cell (asterisk) quickly spread to neighboring cells, whereas coinjected 10-kDa Lucifer Yellow-dextran (yellow) remained within the injected cell. **(B):** In the same field of view, AlexaFluor 488 hydrazide delivered subsequently into a single mouse embryonic fibroblast (MEF) (arrow) quickly spread to other MEFs but not to the adjacent human ES cells. **(C):** Composite of **(A)** and **(B)** with the differential interference contrast (DIC) microscopy image of the same field. **(D, E):** Double immunofluorescence for Oct3/4 **(D)** and human nuclear antigen **(E)** in the same field as **(A–C)**. **(F):** Composite of **(D)** and **(E)** with the DIC image. **(G):** AlexaFluor 568 hydrazide (red) was injected into a single human ES cell (asterisk); AlexaFluor 488 hydrazide (green) was injected into a nearby MEF (arrow). **(H):** Composite of **(G)** and the DIC image of the same field. **(I–L):** Subsequent double immunofluorescence for Oct3/4 and human nuclear antigen. Composite views show the same field as **(G)** and **(H)** with **(I)** or without **(L)** the DIC image. **(M):** AlexaFluor 488 hydrazide (green) was injected into a single MEF (arrow), and AlexaFluor 568 hydrazide (red) was injected into a single human ES cell within a colony. This is the only case that displayed convincing dye spread between the human ES cells and adjacent MEF cells (arrowhead). **(N):** Composite of **(M)** with the DIC image of the same field. Scale bars = 30 um.

cells grown in confluent monolayers. Immediately after attaining the whole cell configuration, the average input resistance was 103 ± 22 MOhm, and the membrane capacitance was 304 ± 102 pF. With internal potassium glucuronate and external Tyrode's solution, the mean zero current potential was –26 ± 1.7 mV. The low input resistance and high membrane capacitance values are consistent with electrical coupling mediated by gap junctions among cells in the monolayer. Because many gap junctions permit the passage of molecules smaller than 1,000 Da, we initially tested for gap junction-mediated dye transfer by including sulforhodamine B (557 Da) within our recording electrodes. As illustrated in Figure 3G, sulforhodamine B readily spread from the recorded cell into neighboring cells of the monolayer. Comparable results were obtained with electrodes that contained Lucifer yellow CH (443 Da; data not shown). To confirm that dye transfer was restricted to low molecular weight compounds, we injected a mixture of low (Alexafluor hydrazide 568; 731 Da) and high (Lucifer Yellow coupled to Dextran; 10 kDa) molecular weight probes into

human ES cells grown as monolayers. The low molecular weight Alexafluor hydrazide passed freely to neighboring cells (Fig. 4A), whereas fluorescent dextran was retained within the injected cell ($n = 15$).

The observation of strong dye coupling between human ES cells under feeder-free conditions led us to test for coupling between human ES cells and adjacent MEF feeder cells. To perform these experiments, individual human ES cells were injected with Alexafluor hydrazide 568 (Fig. 4A, 4C), and single nearby MEFs were injected with Alexafluor hydrazide 488 (570 Da; Fig. 4B, 4C). For some experiments, cultures were fixed after dye injection, and cell identity was subsequently verified by immunofluorescence for Oct3/4 and human nuclear antigen (Fig. 4D–4F, 4I–4L). In all cases ($n = 16$), human-to-human and mouse-to-mouse dye transfer was observed; however, only one clear example was obtained of dye spread from human ES cells to adjacent mouse cells (Fig. 4M, 4N). These experiments confirm strong gap junction-mediated coupling between undifferentiated human ES cells. In contrast, human ES cell coupling to mouse fibroblast feeder cells is extremely rare and is unlikely to be essential for maintenance of human ES cell pluripotency.

Recordings from Coupled Cell Pairs

To evaluate cell-to-cell coupling directly [39, 40], we passaged human ES cells at lower density and used two electrodes to record simultaneously from both cells in isolated pairs that were in contact (Fig. 5). Both of the cells were initially clamped to 0 mV. Currents through gap junctions connecting the two cells were recorded by stepping the potential in one cell to values positive and negative to 0 mV, while maintaining the second cell clamped at 0 mV. This procedure was then repeated with the first cell held at 0 mV and the second cells stepped to different potentials. Such experiments yielded transjunctional conductance values that ranged from 2.7 to 79 nS, with a mean of 20 ± 5 nS ($n = 15$ cell pairs). In all cases, the junctional current reversed polarity at zero transjunctional potential, and there was good agreement in the junctional conductance as determined for steps applied to either of the two cells (Fig. 5E). Linear regression yielded a correlation coefficient of $r = .996$. Current voltage relations for whole cell current and for transjunctional current were relatively linear for transjunctional voltages that ranged from –30 to +30 MV.

Pharmacology of Transjunctional Currents

A number of compounds, including 18-α-glycyrrhetinic acid, long-chain alcohols (e.g., octanol and heptanol), and arylaminobenzoates (e.g., flufenamic acid and niflumic acid), have been shown to reduce cell-to-cell coupling mediated by gap junctions. Although some of these drugs are not entirely specific for gap junction channels [1, 6, 30], they are widely used to identify coupling that is mediated by gap junctions and to probe the functional consequences of pharmacologically induced uncoupling on cell phenotype or survival. We initially tested the effect of 100 μM 18-α-glycyrrhetinic acid [31], flufenamic acid, and niflumic acid [30], as well as 1 mM octanol [1], 2 mM cobalt chloride, and 100 μM lanthanum chloride [1] on the transjunctional conductance between coupled cell pairs (Fig. 6). Lanthanum and cobalt caused no significant change in conductance, whereas all of the organic inhibitors reduced conductance. Onset and recovery of block by flufenamic acid was rapid compared with the slower kinetics observed for octanol, 18-α-glycyrrhetinic, and niflumic acid. These results are broadly consistent with previous pharmacological characterization of native and recombinant gap junction channels [1]. Inhibition of current flow by these compounds, together with the selective passage of low molecular weight dyes described above (Fig. 4A), provides the strongest evidence that the low resistance connections between adjacent cells are formed by gap junctions, rather than by incomplete mitosis or some other type of cytoplasmic continuity.

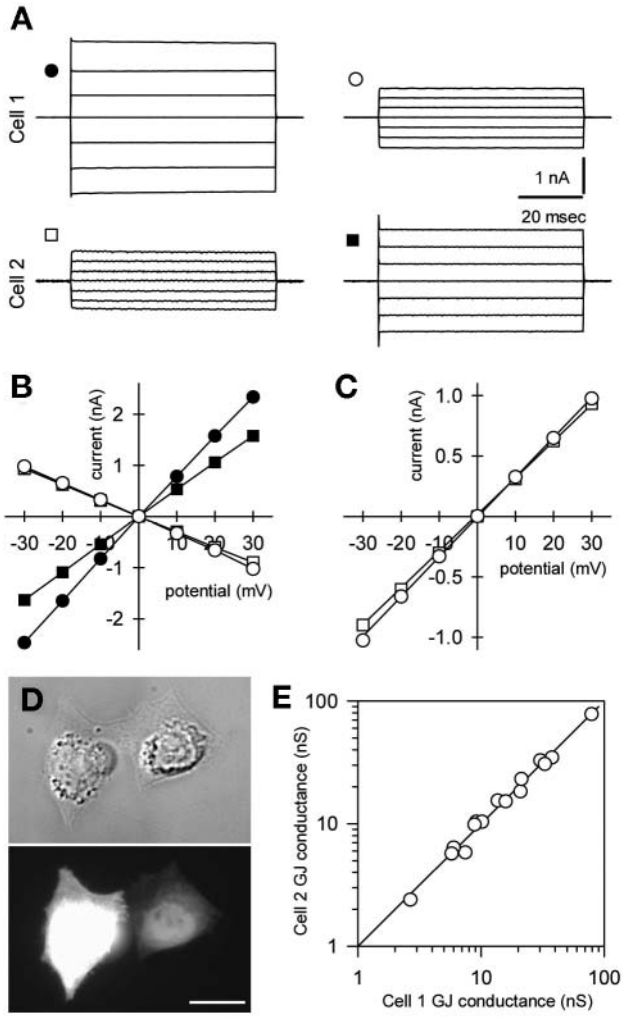

Figure 5. Transjunctional currents recorded from human embryonic stem (ES) cell pairs. **(A):** Whole-cell currents recorded simultaneously from two adjacent human ES cells. Currents were elicited in both cells by voltage steps from –30 to +30 mV delivered either to cell 1 (traces on the left) or to cell 2 (traces on the right). **(B):** Plots of current recorded in cell 1 (circles) or cell 2 (squares) as a function of test potential. Filled symbols indicate that the cell was clamped to the test potential, and open symbols indicate that the cell was clamped to 0 mV. **(C):** Transjunctional current as a function of transjunctional potential. **(D):** Differential interference contrast and fluorescence images of an isolated cell pair that was studied by simultaneous whole-cell recording. Sulforhodamine B was included in the electrode used for the cell on the left. Scale bar = 30 μm. **(E):** Transjunctional conductance as determined by voltage steps applied alternately to both cells of 15 human ES cell pairs. Abbreviation: GJ, gap junction.

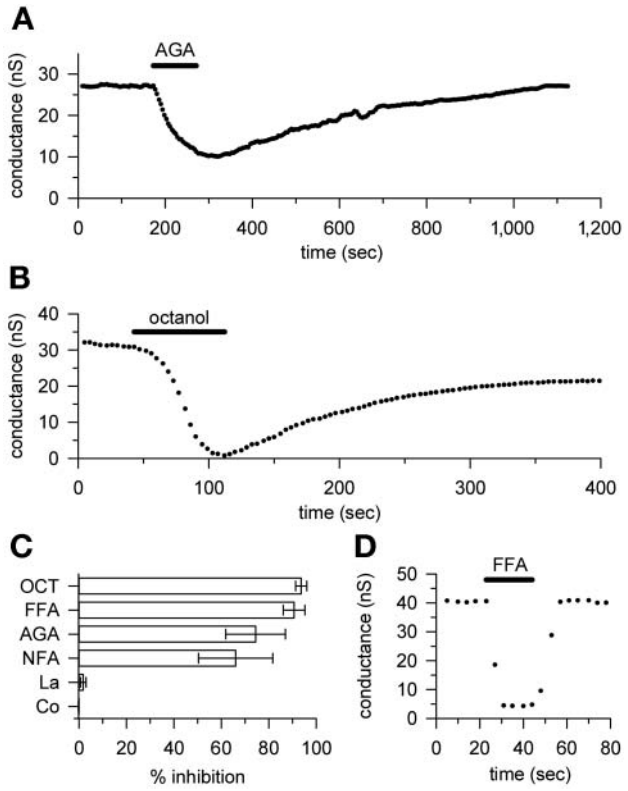

Figure 6. Pharmacology of transjunctional currents recorded from human embryonic stem (ES) cell pairs. **(A):** Transjunctional conductance plotted as a function of time. Period of exposure to 100 μM AGA is indicated by the bar. Conductance was determined from currents evoked when one cell was stepped to +40 mV while the other cell was held at 0 mV. **(B):** Time course of inhibition of transjunctional conductance by 1 mM octanol. **(C):** Mean ± SEM percent inhibition of transjunctional conductance produced by 1 mM OCT, 100 μM FFA, 100 μM AGA, 100 μM NFA, 100 μM La, or 2 mM Co. **(D):** Time course of inhibition of transjunctional conductance by 100 μM FFA. Note: Relative to **(A)**, the time scales are expanded threefold and fivefold in **(B)** and **(D)**, respectively. Abbreviations: AGA, 18 α-glycyrrhetinic acid; Co, cobalt chloride; FFA, flufenamic acid; La, lanthanum chloride; NFA, niflumic acid; OCT, octanol.

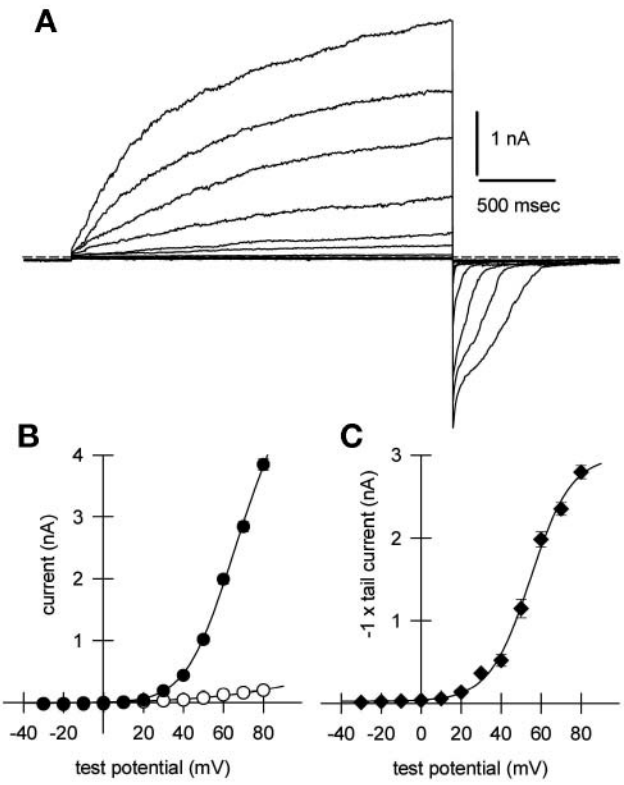

Figure 7. Connexon hemichannel-mediated currents in isolated human embryonic stem (ES) cells. **(A):** Whole-cell currents elicited in an isolated cell by voltage steps from a holding potential of –80 mV to test potentials of –30 to +80 mV. **(B):** Plots of instantaneous (open symbols) and steady-state (filled symbols) currents as a function of test potential. **(C):** Plot of inward tail current recorded at –80 mV (inverted) as a function of the preceding test potential. Smooth curve: best fit of the Boltzmann equation in the form: $I = B/(1 + \exp(-A \times (V_m - V_o))) + C$, where I is the recorded current, V_m is the membrane test potential, and V_o, A, B, and C are fitted parameters. V_o is the potential at half maximal conductance (+55 mV), B and C are the maximal and minimal conductance, respectively, and A can be expressed as zq/kT, where z (best fit = 2.5) is the valence of charge q, k is Boltzmann's constant, and T is the temperature in kelvin.

Connexon-Mediated Currents in Isolated Human ES Cells

In a number of reports, individual isolated cells that are capable of forming gap junctions have been shown to display voltage-dependent hemichannel currents mediated by connexons that have not paired up with a partner on an adjacent cell. Examples include horizontal cells isolated from catfish [41] and skate [42] retina, as well as a variety of cell types maintained in culture. Similarly, recombinant hemichannel-mediated currents have been studied in *Xenopus* oocytes [28, 43] and transfected mammalian cells [44]. Connexins shown to mediate voltage-activated currents include Cx30 [45], Cx43 [29], Cx45 [44], Cx46 [28, 43], and Cx50 [45–47].

To test for the presence of functional hemichannels, we recorded from isolated human ES cells. In contrast to human ES cells growing in monolayers, which display low input resistance owing to the strong coupling to neighboring cells, the isolated human ES cells (n = 31) had significantly higher input resistance (717 ± 111 MOhm, $p < .01$) and lower membrane capacitance (60 ± 5.6 pF, $p = .014$), as well as a less negative mean zero current potential (–16 ± 1.3 mV, $p < .01$). As shown in Figure 7, depolarizing voltage steps evoked slowly activating outward currents with properties similar to those previously described for native and recombinant hemichannels.

In a few cells, the currents activated and decayed along a single exponential time course; however, in most cases, two or more exponentials were required for an adequate fit to activation and deactivation. Moreover, in a number of cells, the activation and deactivation rates exhibited dramatic dependence on the duration that the cell was held at activating or deactivating voltages, which suggests the existence of multiple slowly equilibrating closed and open states. Similar dependence of kinetic parameters on the frequency of stimulation has been reported for recombinant Cx46 hemichannels expressed in *Xenopus* oocytes [28].

Brief voltage steps from holding potentials of –80 or +60 mV (Fig. 8A) were used to evaluate the instantaneous current-voltage (I-V) relation for hemichannel-mediated whole-cell

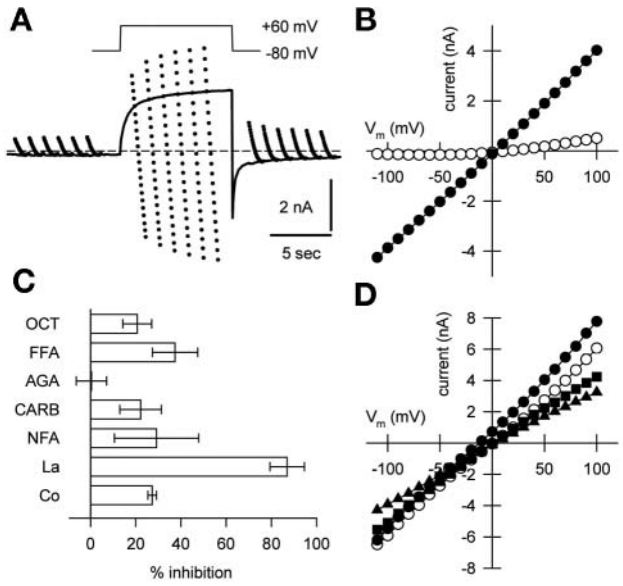

Figure 8. Hemichannel current-voltage relations. **(A):** Whole-cell currents recorded in Tyrode's solution at holding potentials of −80 and +60 mV. The cell was initially held at −80 mV and briefly (15 ms) stepped six times through a series of test potentials ranging from +100 to −110 mV. The holding potential was jumped to +60 mV for 9 seconds, and the series of test potential steps was repeated six times. Finally, the holding potential was returned to −80 mV, and the test potential steps were applied six more times. The solid line plots the holding current. Currents recorded at the end of each test potential step are superimposed as points. Internal solution: 140 mM NMDG, 10 mM HEPES, 0.1 mM EGTA, pH adjusted to 7.4 with HCl. **(B):** Current recorded in **(A)** as a function of test potential for holding potentials of −80 mV (open circles, average of the first six steps to each test potential) and +60 mV (filled circles, average of the last two steps from +60 mV to each test potential). **(C):** Mean ± SEM percent inhibition of hemichannel conductance produced by 1 mM OCT, 100 μM FFA, 100 μM AGA, 100 μM CARB, 100 μM La, or 2 mM Co. **(D):** Current-voltage relations in extracellular NaCl (open circles), *N*-methyl-D-glucamine (NMDG) glucuronate (filled circles), NMDG-chloride (filled squares), and sodium-glucuronate (filled triangles). Internal solution: 140 mM NMDG, 10 mM HEPES, 0.1 mM EGTA, pH adjusted to 7.4 with HCl. Abbreviations: AGA, 18 α-glycyrrhetinic acid; CARB, carbenoxolone; Co, cobalt chloride; FFA, flufenamic acid; La, lanthanum chloride; NFA, niflumic acid; OCT, octanol.

currents. As shown in Figure 8B, the instantaneous *I-V* of open hemichannels was linear and reversed near 0 mV. With external Tyrode's solution, the whole-cell conductance through surface hemichannels in isolated human ES cells ranged from 3.6 to 90.5 nS, with a mean of 40.2 ± 5.6 nS (n = 20 cells). To evaluate the ionic selectivity of channels underlying these currents we substituted large organic cations (NMDG and TEA) or anions (glucuronate) for the small diameter inorganic ions (potassium, cesium, sodium, and chloride) present in our standard intracellular and extracellular solutions. Consistent with the nonselective permeation properties of connexons, we observed relatively linear *I-V* relations, which reversed between –10 and +10 mV, using a variety of different internal and external solutions (Fig. 8D). These included internal solutions containing potassium glucuronate, cesium glucuronate, NMDG-chloride, or TEA-chloride as the major intracellular salts, and paired with NaCl, NMDG-chloride, sodium glucuronate, or NMDG-glucuronate as the major extracellular salts (Materials and Methods). The linear instantaneous *I-V* relations, and the lack of any dramatic change in potential at which current reversed polarity, indicate that the large organic ions pass through the channels as readily as the smaller inorganic ions. This stands in contrast to most conventional voltage-gated channels, which typically are selective for smaller inorganic ions [27].

Consistent with previous work [28, 29], lanthanum and cobalt strongly blocked the currents mediated by hemichannels (Fig. 8C). Organic antagonists also affected connexons (Fig. 8C); however, the inhibition was relatively weaker than for transjunctional current through gap junctions (Fig. 6C). Studies of recombinant hemichannels [6, 48] have demonstrated that connexons are not all equally sensitive to block by organic gap junction antagonists, which suggests that human ES cell hemichannels may include individual connexins, or connexin combinations, that are relatively resistant to inhibition by the organic blockers.

Evaluation of Junctional Versus Nonjunctional Connexin Distribution in Cell Pairs

It is of interest to ask whether the hemichannel-mediated currents recorded in isolated cells simply reflect the absence of a suitable partner for cell-to-cell junction formation or whether cells that have formed junctions with their neighbors might retain a significant proportion of unpaired connexons on their surface. To evaluate this question, we again recorded from pairs of cells, but both cells were stepped simultaneously to the same positive potential, relative to the bath. This protocol will maintain the transjunctional voltage at 0 mV and hence eliminate junctional current. Out of 22 cells (11 pairs) tested in this way, six cells displayed slowly activating outward currents characteristic of connexon hemichannels, and all six of these cells were paired with a cell that lacked hemichannel-mediated current. In these six cells, the ratio of surface hemichannel conductance to transjunctional conductance ranged from 0.36 to 2.1, with a mean of 1.14 ± 0.32 (n = 6 cells). Linear regression for hemichannel conductance and transjunctional conductance yielded a correlation coefficient of r = .742. These results suggest that connexons preferentially combine to form gap junctions, but hemichannels will be present in cells that express an excess of connexons, outnumbering the available partners on neighboring cells.

Dye Loading Through Surface Membrane Hemichannels

In addition to depolarizing voltage steps, opening of cell surface hemichannels is favored by removal of extracellular calcium [28, 41]. As shown in Figure 9A and 9B, local perfusion of isolated human ES cells with calcium-free external solution evoked a reversible increase in conductance. Previous studies have shown that cells expressing hemichannels on their surface membrane can be loaded with dye dissolved in calcium-free medium [49]. To determine whether hemichannels were present on the surface of human ES cells in high-density monolayers, we exposed cells to sulforhodamine B or propidium iodide in calcium-free Tyrode's solution. As demonstrated in Figure 9C–9F, a subset of cells contained the dye after a brief incubation in calcium-free, but not in calcium-containing, solutions. As mentioned

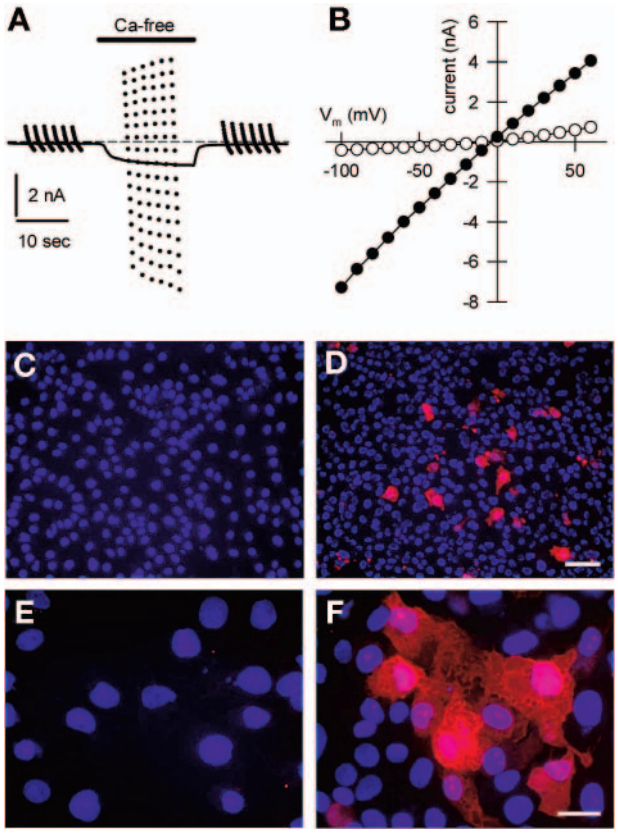

Figure 9. Conductance and dye loading through surface membrane hemichannels in calcium-free medium. **(A):** Whole-cell current evoked by calcium-free external solution in an isolated human embryonic stem (ES) cell. The cell was held at –20 mV in NaCl external solution and briefly (40 ms) stepped six times through a series of test potentials from +60 to –100 mV. Calcium-free external solution was applied by local perfusion and the series of test potential steps was repeated, followed by recovery. **(B):** Current recorded in **(A)** as a function of test potential in control NaCl (open circles, average of the first six steps to each test potential) and calcium-free (filled circles, average of the last two steps to each test potential) external solution. Undifferentiated human ES cell cultures were exposed to propidium iodide in Tyrode's solution containing 2 mM calcium **(C, E)** or 0 mM calcium **(D, F)** for 15 minutes in the dark, rinsed, and observed immediately. Photomicrographs were taken after brief fixation and incubation with Hoechst 33258. Scale bars = **(C, D)**, 100 μm; **(E, F)**, 30 μm.

above, our recordings from cell pairs suggest that hemichannels are present on cells that express a higher number of connexons than their nearest neighbors. Thus, the uneven distribution of dye uptake is likely to reflect the location of cells with a higher relative level of connexin expression than surrounding cells.

Discussion

ES cells are derived from the inner cell mass, a cluster of cells that display extensive gap junction-mediated coupling in early human embryos [50–52]. Our results show that connexin expression and gap junction coupling are maintained in human ES cells propagated in vitro. Recordings from isolated cell pairs provide direct evidence for the formation of functional gap junction communication pathways between human ES cells in culture. Brief steps of transjunctional voltage elicited linear currents between the cells. Conductance across the junctions varied from approximately 3 to approximately 80 ns among the cell pairs sampled. In theory, low resistance coupling might arise as an artifact of incomplete cell division or some other form of cytoplasmic continuity. However, strong confirmation that gap junctions underlie the conductance between adjacent cells comes from the reversible blockade by pharmacological agents known to inhibit gap junction channels and from the failure of high molecular weight fluorescent dextran to spread from injected cells.

Mammalian embryos express a large number of different connexins. Studies in rodents have reported zygotic expression of transcripts for Cx30, Cx31, Cx31.1, Cx36, Cx40, Cx43, Cx45, and Cx57 [7, 53–55]. Zygotic transcription of Cx26 and Cx32 cannot be detected in mouse embryos [53, 54], although Cx32 protein of maternal origin persists in mice up to implantation [56]. In contrast, rat embryos transcribe Cx26 [55], raising the possibility of species variability in the profile of connexin expression. Our results in human ES cells are broadly consistent with these studies on the embryonic pattern of connexin expression and with earlier brief reports of evidence for Cx43 and Cx45 expression by mouse [14] and human [15–17] ES cells. Transcripts for Cx40.1 and Cx50 were not observed in human ES cells by RT-PCR, whereas PCR products for Cx25, Cx26, Cx30.3, Cx31, Cx31.1, Cx31.9, Cx37, Cx40, Cx43, Cx45, and Cx46 were detected for all human ES cultures sampled, and somewhat weaker or more variable expression was detected for Cx30, Cx30.2, Cx32, Cx36, Cx47, Cx59, and Cx62. Consistent with prior immunofluorescent visualization of connexins in human embryos [51, 52], antibodies to Cx40, Cx43, and Cx45 labeled points of contact between adjacent human ES cells. Thus, undifferentiated human ES cells express most of the known connexins at the level of RNA, and at least some of these are translated into protein and delivered to the surface membrane at points of intercellular contact.

Cell-to-cell coupling via gap junctions is a common feature of embryonic development, although the role of embryonic cell junctions remains elusive. Direct evidence for electrical coupling among embryonic cells was first described in squid embryos [57] and was subsequently demonstrated in a variety of other species. In both mouse [58–60] and human [51] embryos, organization of connexins into gap junctions can be visualized morphologically, beginning at the four- to eight-cell stage. In mouse embryos, evidence for functional coupling can first be obtained at the eight-cell stage [3], whereas in human embryos, extensive dye coupling arises somewhat later [50]. Initially, all cells within the embryo are coupled electrically, and dye injected into one cell quickly spreads to all others. As differentiation proceeds, there is a progressive loss of communication between different tissues [3, 9], whereas coupling within a given compartment remains strong. For example, following implantation, cells in the inner cell mass remain well coupled, but spread of fluorescent dye to the surrounding trophoblast diminishes [3]. Similarly, cells within each of the early germ layers remain coupled to each other, whereas dye fails to spread across the boundaries between germ layers. Electrical coupling may persist after dye coupling has been lost [3, 9], but there is clearly a change in communication as tissues differentiate in

vivo. In human ES cell monolayer cultures, dye injected into individual cells spreads quickly and uniformly to all surrounding cells. Therefore, cultured human ES cells remain extensively coupled through repeated passages, preserving the communication pathways that exist within the inner cell mass. In mixed cultures that included both human ES cells and mouse embryonic fibroblast feeder cells, we observed dye coupling within each population; however, coupling between human ES and MEF cells was extremely rare. These results suggest that preservation of human ES cell pluripotency does not require direct transmission of signals from MEF cells to human ES cells via gap junction channels, but they leave open the possibility that coupling between adjacent human ES cells may play a role in coordinating cellular responses to external signals that maintain pluripotency or that stimulate differentiation.

Indeed, the function of embryonic cell-to-cell communication has not been determined [61]. Single and double knockout mice, which lack one or more individual connexins, exhibit relatively normal early development [62–65], although compensation by other connexins expressed in the embryo might explain the lack of an obvious phenotype prior to implantation. Several early reports provided evidence for developmental abnormalities following acute blockade of embryonic gap junctions by injection of blocking antibodies [66] or connexin antisense RNA [67]. More recent pharmacological work has tested the effect of chronic exposure to the gap junction inhibitor 18-alpha glycyrrhetinic acid. Studies of intact or chimeric mouse inner cell mass reported essentially normal differentiation up to the blastocyst stage during continuous exposure to the drug [55, 68]. On the other hand, 18-α glycyrrhetinic acid was found to inhibit in vitro differentiation of human NT2/D1 cells [69], which are multipotent teratocarcinoma cells that share a number of properties with pluripotent ES cells. In addition, recent studies of transformed cell lines have raised the possibility that Cx43 may have growth regulatory effects that are independent of its ability to form functional gap junctions [70, 71]. Clearly, the functional implications of connexin expression on human ES cell growth and differentiation merit further investigation.

Previous studies in both native and recombinant systems have documented a number of differences in the properties of gap junctions or hemichannels formed by different connexins, including differences in kinetics, unitary conductance, and permeability for specific dyes [45, 72, 73]. The large number of connexin RNAs expressed in embryos and human ES cells suggests that, in both cases, the cells may produce heteromeric connexons containing two or more distinct connexin subunits. Further work will be needed to quantify the relative connexin protein levels and to determine the stoichiometry of connexins that combine to form connexon hexamers in these cells.

In general, strong depolarization or reduction in extracellular calcium promotes the opening of surface membrane hemichannels [28, 41]. Prolonged depolarization of human ES cells to membrane potentials of +30 mV or greater elicited slowly activating outward currents typical of connexon hemichannels. The nonselective nature of this conductance was verified by comparing instantaneous *I-V* relations for internal and external solutions of diverse composition. For all solutions tested, the current evoked by holding at positive potentials was essentially linear and reversed between –10 and +10 mV, indicating similar permeability to both small inorganic and larger organic ions. Removal of extracellular calcium produced a significant increase in membrane conductance and allowed for dye entry from the extracellular medium, consistent with opening of surface hemichannels in calcium-free solutions, as observed in other cell types [49]. In medium that contained 1–2 mM calcium, currents through human ES cell hemichannels were minimal when cells were maintained at their normal zero current potential between –15 and –30 mV, suggesting that most hemichannels remain closed in cells at rest.

Investigation of human ES cells is still at an early stage. Identifying characteristics of human ES cells are currently limited to the expression of a few relatively specific markers and the ability to differentiate into cells from all three germ layers. The gold standard for proof of an undifferentiated nonhuman embryonic stem cell phenotype is the ability to generate a chimeric animal following injection into the blastocyst inner cell mass. This of course is not a testable option for human ES cells. Our data provide additional ultrastructural, immunocytochemical, and physiological properties that may aid in proper confirmation of undifferentiated human ES cells. In addition to expression of the Oct3/4, SSEA-3, SSEA-4, TRA-1-60, and TRA-1-81 antigens, the expression profile for connexins (positive for Cx25, Cx26, Cx30.3, Cx31, Cx31.1, Cx31.9, Cx37, Cx40, Cx43, Cx45, and Cx46; negative for Cx40.1 and Cx50) and physiological dye coupling can be added to the growing list of human ES cell characteristics in the undifferentiated state. Collectively, our results establish human ES cells as a good model system for the investigation of direct intercellular communication channels during early stages of differentiation.

ACKNOWLEDGMENTS

We are grateful to Tim Wilding for technical assistance and Dr. Tom Steinberg for generously providing anti-Cx45 antibodies. This work was supported by grants from the NIH (NS045023 to J.E.H.; NS39577 and NS40520 to J.W.M.), the Sam Schmidt Race for a Cure Foundation, and the Jack Orchard ALS Foundation.

DISCLOSURES

The authors indicate no potential conflicts of interest.

REFERENCES

1 Saez JC, Berthoud VM, Branes MC et al. Plasma membrane channels formed by connexins: Their regulation and functions. Physiol Rev 2003; 83:1359–1400.

2 White TW, Paul DL. Genetic diseases and gene knockouts reveal diverse connexin functions. Annu Rev Physiol 1999;61:283–310.

3 Lo CW, Gilula NB. Gap junctional communication in the preimplantation mouse embryo. Cell 1979;18:399–409.

4 Lo CW, Gilula NB. Gap junctional communication in the post-implantation mouse embryo. Cell 1979;18:411–422.

5 Willecke K, Eiberger J, Degen J et al. Structural and functional diversity of connexin genes in the mouse and human genome. Biol Chem 2002; 383:725–737.

6 Goodenough DA, Paul DL. Beyond the gap: Functions of unpaired connexon channels. Nat Rev Mol Cell Biol 2003;4:285–294.

7 Reuss B, Hellmann P, Traub O et al. Expression of connexin31 and connexin43 genes in early rat embryos. Dev Genet 1997;21:82–90.

8 Davies TC, Barr KJ, Jones DH et al. Multiple members of the connexin gene family participate in preimplantation development of the mouse. Dev Genet 1996;18:234–243.

9 Kalimi GH, Lo CW. Communication compartments in the gastrulating mouse embryo. J Cell Biol 1988;107:241–255.

10 Gossler A, Joyner AL, Rossant J et al. Mouse embryonic stem cells and reporter constructs to detect developmentally regulated genes. Science 1989;24:463–465.

11 Suda Y, Suzuki M, Ikawa Y et al. Mouse embryonic stem cells exhibit indefinite proliferative potential. J Cell Physiol 1987;133:197–201.

12 Thomson JA, Itskovitz-Eldor J, Shapiro SS et al. Embryonic stem cell lines derived from human blastocysts. Science 1998;282:1145–1147.

13 Donovan PJ, Gearhart J. The end of the beginning for pluripotent stem cells. Nature 2001;414:92–97.

14 Oyamada Y, Komatsu K, Kimura H et al. Differential regulation of gap junction protein (connexin) genes during cardiomyocytic differentiation of mouse embryonic stem cells in vitro. Exp Cell Res 1996;229:318–326.

15 Bhattacharya B, Miura T, Brandenberger R et al. Gene expression in human embryonic stem cell lines: Unique molecular signature. Blood 2004;103:2956–2964.

16 Carpenter MK, Rosler ES, Fisk GJ et al. Properties of four human embryonic stem cell lines maintained in a feeder-free culture system. Dev Dyn 2004;229:243–258.

17 Richards M, Tan SP, Tan JH et al. The transcriptome profile of human embryonic stem cells as defined by SAGE. STEM CELLS 2004;22:51–64.

18 Abbondanzo SJ, Gadi I, Stewart CL. Derivation of embryonic stem cell lines. Methods Enzymol 1993;225:803–823.

19 Reubinoff BE, Pera MF, Fong CY et al. Embryonic stem cell lines from human blastocysts: Somatic differentiation in vitro. Nat Biotechnol 2000;18:399–404.

20 Amit M, Carpenter MK, Inokuma MS et al. Clonally derived human embryonic stem cell lines maintain pluripotency and proliferative potential for prolonged periods of culture. Dev Biol 2000;227:271–278.

21 Mitalipova M, Calhoun J, Shin S et al. Human embryonic stem cell lines derived from discarded embryos. STEM CELLS 2003;21:521–526.

22 Zeng X, Miura T, Luo Y et al. Properties of pluripotent human embryonic stem cells BG01 and BG02. STEM CELLS 2004;22:292–312.

23 Xu C, Inokuma MS, Denham J et al. Feeder-free growth of undifferentiated human embryonic stem cells. Nat Biotechnol 2001;19:971–974.

24 Di W-L, Rugg EL, Leigh IM et al. Multiple epidermal connexins are expressed in different keratinocyte subpopulations including connexin 31. J Invest Dermatol 2001;117:958–964.

25 Johnson CM, Kanter EM, Green KG et al. Redistribution of connexin45 in gap junctions of connexin43-deficient hearts. Cardiovasc Res 2002;53:921–935.

26 Lecanda F, Towler DA, Ziambaras K et al. Gap junctional communication modulates gene expression in osteoblastic cells. Mol Biol Cell 1998;9:2249–2258.

27 Hille B. Ion Channels of Excitable Membranes, 3rd ed. Sunderland, MA: Sinauer, 2001.

28 Ebihara L, Steiner E. Properties of a nonjunctional current expressed from a rat connexin 46 cDNA in *Xenopus* oocytes. J Gen Physiol 1993;102:59–74.

29 Contreras JE, Saez JC, Bukauskas FF. Gating and regulation of connexin 43 (Cx43) hemichannels. Proc Natl Acad Sci U S A 2003;100:11388–11393.

30 Harks EG, de Roos AD, Peters PH et al. Fenamates: A novel class of reversible gap junction blockers. J Pharmacol Exp Ther 2001;298:1033–1041.

31 Davidson JS, Baumgarten IM. Glycyrrhetinic acid derivatives: A novel class of inhibitors of gap-junctional intercellular communication. Structure-activity relationships. J Pharmacol Exp Ther 1988;246:1104–1107.

32 Carpenter MK, Inokuma MS, Denham J et al. Enrichment of neurons and neural precursors from human embryonic stem cells. Exp Neurol 2001;172:383–397.

33 Henderson JK, Draper JS, Baillie HS et al. Preimplantation human embryos and embryonic stem cells show comparable expression of stage-specific embryonic antigens. STEM CELLS 2002;20:329–337.

34 Okamoto K, Okazawa H, Okuda A et al. A novel octamer binding transcription factor is differentially expressed in mouse embryonic cells. Cell 1990;60:461–472.

35 Rosner MH, Vigano MA, Ozato K et al. A POU-domain transcription factor in early stem cells and germ cells of the mammalian embryo. Nature 1990;345:686–692.

36 Yeom YI, Fuhrmann G, Ovitt CE et al. Germline regulatory element of Oct-4 specific for the totipotent cycle of embryonal cells. Development 1996;122:881–894.

37 Zhang SC, Wernig M, Duncan ID et al. In vitro differentiation of transplantable neural precursors from human embryonic stem cells. Nat Biotechnol 2001;19:1129–1133.

38 Revel J-P, Karnovsky MJ. Hexagonal array of subunits in intercellular junctions of the mouse heart and liver. J Cell Biol 1967;33:C7–C12.

39 Neyton J, Trautmann A. Single-channel currents of an intercellular junction. Nature 1985;317:331–335.

40 White RL, Spray DC, Campos de Carvalho AC et al. Some electrical and pharmacological properties of gap junctions between adult ventricular myocytes. Am J Physiol 1985;249:C447–C455.

41 DeVries SH, Schwartz EA. Hemi-gap-junction channels in solitary horizontal cells of the catfish retina. J Physiol 1992;445:201–230.

42 Malchow RP, Qian H, Ripps H. Evidence for hemi-gap junctional channels in isolated horizontal cells of the skate retina. J Neurosci Res 1993;35:237–245.

43 Paul DL, Ebihara L, Takemoto LJ et al. Connexin 46, a novel lens gap junction protein, induces voltage-gated currents in nonjunctional plasma membrane of *Xenopus* oocytes. J Cell Biol 1991;115:1077–1089.

44 Valiunas V. Biophysical properties of connexin-45 gap junction hemichannels studied in vertebrate cells. J Gen Physiol 2002;119:147–164.

45 Valiunas V, Weingart R. Electrical properties of gap junction hemichannels identified in transfected HeLa cells. Pflugers Arch 2000;440:366–379.

46 Beahm DL, Hall JE. Hemichannel and junctional properties of connexin 50. Biophys J 2002;82:2016–2031.

47 Srinivas M, Costa M, Gao Y et al. Voltage dependence of macroscopic and unitary currents of gap junction channels formed by mouse connexin50 expressed in rat neuroblastoma cells. J Physiol 1999;517:673–689.

48 Eskandari S, Zampighi GA, Leung DW et al. Inhibition of gap junction hemichannels by chloride channel blockers. J Membr Biol 2002;185:93–102.

49 Li H, Liu TF, Lazrak A et al. Properties and regulation of gap junctional hemichannels in the plasma membranes of cultured cells. J Cell Biol 1996;134:1019–1030.

50 Dale B, Gualtieri R, Talevi R et al. Intercellular communication in the early human embryo. Mol Reprod Dev 1991;29:22–28.

51 Hardy K, Warner A, Winston RM. Expression of intercellular junctions during preimplantation development of the human embryo. Mol Hum Reprod 1996;2:621–632.

52 Bloor DJ, Wilson Y, Kibschull M et al. Expression of connexins in human preimplantation embryos in vitro. Reprod Biol Endocrinol 2004;2:25.

53 Nishi M, Kumar NM, Gilula NB. Developmental regulation of gap junction gene expression during mouse embryonic development. Dev Biol 1991;146:117–130.

54 Valdimarsson G, De Sousa PA, Beyer EC et al. Zygotic expression of the connexin43 gene supplies subunits for gap junction assembly during mouse preimplantation development. Mol Reprod Dev 1991;30:18–26.

55 Houghton FD, Barr KJ, Walter G et al. Functional significance of gap junctional coupling in preimplantation development. Biol Reprod 2002; 66:1403–1412.

56 Barron DJ, Valdimarsson G, Paul DL et al. Connexin32, a gap junction protein, is a persistent oogenetic product through preimplantation development of the mouse. Dev Genet 1989;10:318–323.

57 Potter DD, Furshpan EJ, Lennox ES. Connections between cells of the developing squid as revealed by electrophysiological methods. Proc Natl Acad Sci U S A 1966;55:328–336.

58 De Sousa PA, Valdimarsson G, Nicholson BJ et al. Connexin trafficking and the control of gap junction assembly in mouse preimplantation embryos. Development 1993;117:1355–1367.

59 Becker DL, Evans WH, Green CR et al. Functional analysis of amino acid sequences in connexin43 involved in intercellular communication through gap junctions. J Cell Sci 1995;108:1455–1467.

60 Dahl E, Winterhager E, Reuss B et al. Expression of the gap junction proteins connexin31 and connexin43 correlates with communication compartments in extraembryonic tissues and in the gastrulating mouse embryo, respectively. J Cell Sci 1996;109:191–197.

61 Kidder GM, Winterhager E. Intercellular communication in preimplantation development: The role of gap junctions. Front Biosci 2001;6: D731–D736.

62 De Sousa PA, Juneja SC, Caveney S et al. Normal development of preimplantation mouse embryos deficient in gap junctional coupling. J Cell Sci 1997;110:1751–1758.

63 Houghton FD, Thonnissen E, Kidder GM et al. Doubly mutant mice, deficient in connexin32 and -43, show normal prenatal development of organs where the two gap junction proteins are expressed in the same cells. Dev Genet 1999;24:5–12.

64 Krüger O, Plum A, Kim JS et al. Defective vascular development in connexin 45-deficient mice. Development 2000;127:4179–4193.

65 Kumai M, Nishii K, Nakamura K et al. Loss of connexin45 causes a cushion defect in early cardiogenesis. Development 2000;127:3501–3512.

66 Lee S, Gilula NB, Warner AE. Gap junctional communication and compaction during preimplantation stages of mouse development. Cell 1987;51:851–860.

67 Bevilacqua A, Loch-Caruso R, Erickson RP. Abnormal development and dye coupling produced by antisense RNA to gap junction protein in mouse preimplantation embryos. Proc Natl Acad Sci U S A 1989;86: 5444–5448.

68 Vance MM, Wiley LM. Gap junction intercellular communication mediates the competitive cell proliferation disadvantage of irradiated mouse preimplantation embryos in aggregation chimeras. Radiat Res 1999;152: 544–551.

69 Bani-Yaghoub M, Bechberger JF, Underhill TM et al. The effects of gap junction blockage on neuronal differentiation of human NTera2/clone D1 cells. Exp Neurol 1999;156:16–32.

70 Moorby C, Patel M. Dual functions for connexins: Cx43 regulates growth independently of gap junction formation. Exp Cell Res 2001; 271:238–248.

71 Zhang YW, Kaneda M, Morita I. The gap junction-independent tumor-suppressing effect of connexin 43. J Biol Chem 2003;278:44852–44856.

72 Ebihara L, Berthoud VM, Beyer EC. Distinct behavior of connexin56 and connexin46 gap junctional channels can be predicted from the behavior of their hemi-gap-junctional channels. Biophys J 1995;68: 1796–1803.

73 Elfgang C, Eckert R, Lichtenberg-Frate H et al. Specific permeability and selective formation of gap junction channels in connexin-transfected HeLa cells. J Cell Biol 1995;129:805–817.